Neutron Diffraction and Ab initio Studies of Te Site Preference in $Mo_3Sb_{7-x}Te_x$

Christophe Candolfi,*,† Bertrand Lenoir,† Anne Dauscher,† Janusz Tobola,‡ Simon J. Clarke,§ and Ron I. Smith||

Laboratoire de Physique des Matériaux, UMR 7556, Ecole Nationale Supérieure des Mines de Nancy, Parc de Saurupt, 54042 Nancy Cedex, France, Faculty of Physics and Applied Computer Science, AGH University of Science and Technology, 30-059 Krakow, Poland, Inorganic Chemistry Laboratory, Department of Chemistry, University of Oxford, South Parks Road, Oxford OXI 3 QR, United Kingdom, and ISIS Facility, Rutherford Appleton Laboratory, Chilton, Didcot, Oxon OX11 0QX, United Kingdom

Received June 10, 2008. Revised Manuscript Received July 25, 2008

Band structure calculations based on the KKR-CPA method have been undertaken on the $Mo_3Sb_{7-x}Te_x$ and $Re_3As_{7-x}Ge_x$ systems as well as neutron diffraction analysis on the polycrystalline Mo_3Sb_7 and $Mo_3Sb_{5.4}Te_{1.6}$ compounds. Both results strongly suggest that the Te atoms are located only on the 12*d* crystallographic site, whereas the Ge atoms are located on the 16f site as previously experimentally underlined from neutron diffraction study. From an electronic point of view, this site preference in the $Mo_3Sb_{7-x}Te_x$ samples is well-supported by total energy estimation and is presumably related to the reduction of the overall valence p states of Te with respect to those of the 12d Sb site.

1. Introduction

Huge efforts have been made in the past decade to identify new thermoelectric materials for refrigeration and power generation applications.[1−5] To be an efficient converter, a thermoelectric material should exhibit a high dimensionless figure of merit, *ZT*, expressed as[6]

$$ZT = \frac{\alpha^2}{\rho\lambda}T \qquad (1)$$

where α is the Seebeck coefficient or thermoelectric power, ρ the electrical resistivity, λ the total thermal conductivity composed of two terms: the lattice thermal conductivity λ_L and the carrier thermal conductivity λ_e, and *T* the absolute temperature. This equation clearly shows how tough the task is, as a good candidate must conduct electricity like a crystal and impede phonon transport, e.g., have a glasslike behavior.[7] To achieve low thermal conductivity values, complex crystalline structures or compounds with weakly bounded atoms in oversized cages have been extensively studied.[1,2,8−12] The former should bring low lattice thermal conductivity values via strong disorder and mass fluctuations, whereas the latter can rattle about their equilibrium position in their cages, disrupting harmonic modes of the parent atoms. The challenge then lies in maintaining low electrical resistivity. That is why narrow band gap semiconductors and semimetals with a small band overlap stand for the best candidates.

Recently, it was shown that some compounds based on M_3X_7 and crystallizing in the Ir_3Ge_7-type structure can exhibit exotic phenomena at low temperature[13−15] while they can be promising materials for power generation at high temperature.[16,17] In the M_3X_7 structure, M is preferentially 4d and 5d transition metals whereas X can be either the triels Ga and In, the tetrels Ge and Sn, or the pentels As and Sb. The crystal structure of the binary compound M_3X_7 (space group *Im3m*, No. 229) is body-centered cubic and consists of an ensemble of two condensed antiprisms, sharing a square face formed by metalloid atoms (Figure 1a). The M atoms sit at the center of these fundamental building blocks. The rotation angle between square faces is 45° whatever the compound is, resulting in two inequivalent sites for X atoms. The first one situated at the shared square face denotes the X1 (12d) positions, whereas the X atoms defining the

* Corresponding author. E-mail: candolfi@mines.inpl-nancy.fr.
† Ecole Nationale Supérieure des Mines de Nancy.
‡ AGH University of Science and Technology, Krakow.
§ University of Oxford.
|| Rutherford Appleton Laboratory.

(1) Tritt, T. M. *Science* **1999**, *283*, 804–805.
(2) DiSalvo, F. J. *Science* **1999**, *285*, 703–706.
(3) Dauscher, A. Lenoir, B. Scherrer, H.; Caillat, T. *Recent Research Development in Materials Science*; Research Signpost: Kerala, India, 2002; Vol. 3, pp 180−207.
(4) Rowe, D. M. *Thermoelectrics Handbook: Macro to Nano*; CRC Taylor & Francis: Boca Raton, FL, 2006.
(5) Snyder, G. J.; Toberer, E. S. *Nat. Mater.* **2008**, *7*, 105–114.
(6) Ioffe, A. F. *Physics of Semiconductors*; Academic Press: New York, 1960.
(7) Slack, G. A. In *CRC Handbook of Thermoelectrics*; CRC Press: Boca Raton, FL, 1995; Section *D*, p 34.
(8) Brown, S. R.; Kauzlarich, S. M.; Gascoin, F.; Snyder, G. J. *Chem. Mater.* **2006**, *18*, 1873–1877.
(9) Brown, S. R.; Toberer, E. S.; Ikeda, T.; Cox, C. A.; Gascoin, F.; Kauzlarich, S. M.; Snyder, G. J. *Chem. Mater.* **2008**, *20*, 3412–3419.
(10) Sales, B. C.; Mandrus, D.; Williams, R. K. *Science* **1996**, *272*, 1325–1328.
(11) Uher, C. *Semicond. Semimet.* **2001**, *69*, 139, and references therein.
(12) Nolas, G. S.; Cohn, J. L.; Slack, G. A.; Schujman, S. B. *Appl. Phys. Lett.* **1998**, *73*, 178–180.
(13) Candolfi, C.; Lenoir, B.; Dauscher, A.; Bellouard, C.; Hejtmanek, J.; Santava, E.; Tobola, J. *Phys. Rev. Lett.* **2007**, *99*, 037006.
(14) Tran, V. H.; Miiller, W.; Bukowski, Z. *Phys. Rev. Lett.* **2008**, *100*, 137004.
(15) Candolfi, C.; Lenoir, B.; Dauscher, A.; Hejtmanek, J.; Santava, E.; Tobola, J. *Phys. Rev. B* **2008**, *77*, 092509.
(16) Dashjav, E.; Szczepenowska, A.; Kleinke, H. *J. Mater. Chem.* **2002**, *12*, 345–349.
(17) Gascoin, F.; Rasmussen, J.; Snyder, G. J. *J. Alloys Compd.* **2007**, *427*, 324–329.

10.1021/cm801560n CCC: $40.75
Published on Web 09/25/2008

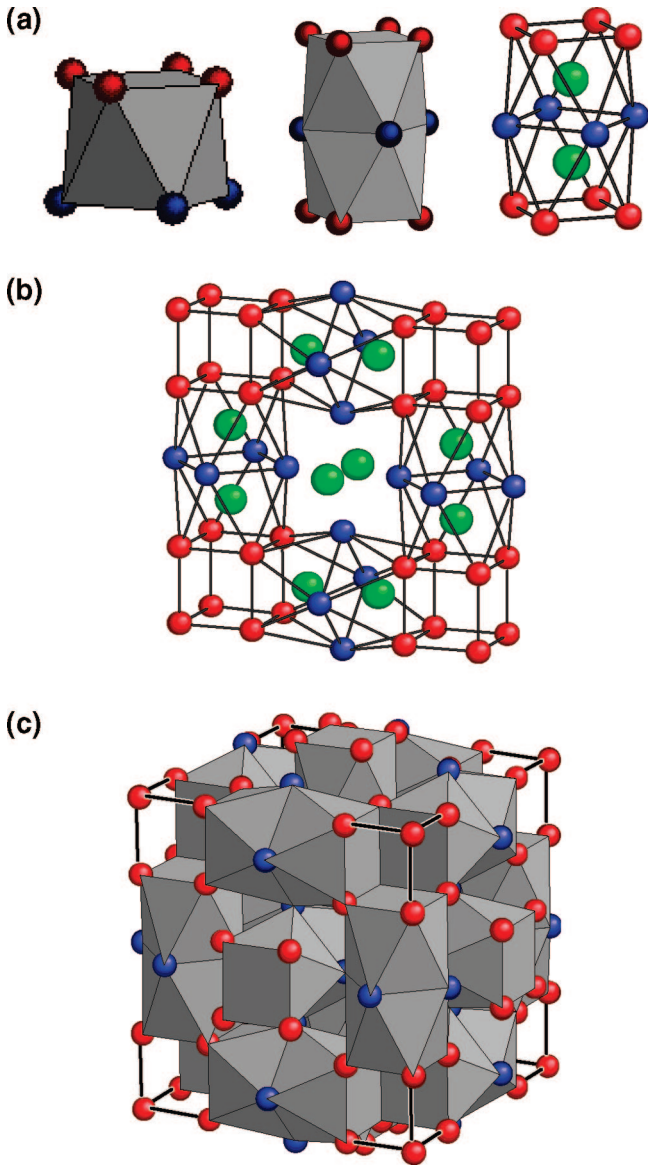

Figure 1. (a) Antiprisms formed by four Sb1 atoms (in blue) and eight Sb2 atoms (in red). The Mo atoms (in green) sit at the center of each prism. (b) Structural blocks to highlight the empty cube. (c) Unit cell of the binary Mo_3Sb_7 compound.

opposite square faces correspond to the second site (16f), called X2. These units are joined together to a framework by sharing common edges of the terminal square faces and determine the empty cube surrounded by 8 X2 atoms as shown in Figure 1b. The center of this cavity represents the site 2a (0, 0, 0). The size of the cavity is governed both by the x parameter of the site 16f (x, x, x), positioning the X2 atoms and the lattice parameter a. Finally, the cubic unit cell of the M_3X_7 compound assembles the aforementioned blocks in such a way that the centers of the empty cubes are placed at the origin of the cell (Figure 1c).

First theoretical studies performed by Häussermann et al.[18] shed some light on this family by suggesting that binary compounds exhibiting strong d−p interactions should be semiconducting when the number of valence electrons equals 55 per M_3X_7 formula unit (i.e., VEC = 55). Later, these assumptions were theoretically confirmed from LMTO calculations in both the $Mo_3Sb_{7-x}Te_x$ and $Re_3As_{7-x}Ge_x$ systems, where the semiconducting state was predicted for $x = 2$ and $x = 1$, respectively.[15,19] Although these studies showed well that the former compound should display a p-type behavior whereas the latter should exhibit n-type character, no detailed analysis has been made on the chemical disorder present in the crystalline structure of $Mo_3Sb_{7-x}Te_x$. Because the transport properties are highly dependent on the band structure near the Fermi level, it is of prime importance from a fundamental point of view but also for experimentators to have an accurate electronic band structure description when Sb or As are replaced by Te or Ge. More precisely, these substitutions raise the question whether Te and Ge atoms can be located only on either the 12d or the 16f site or on both sites. It is interesting to notice that a 16f site preference of the Ge atoms in the $Re_3As_{7-x}Ge_x$ system has been unambiguously demonstrated from neutron diffraction experiments as a result of the larger difference in the neutron scattering factors (As: +6.58 fm and Ge: +8.19 fm).[19] In the case of the $Mo_3Sb_{7-x}Te_x$ system, the 12d site preference of the Te atoms has been only postulated on the basis of electronegativity considerations, but neither experimental nor theoretical evidence have been advanced to ascertain this site preference.[16]

The aim of this paper is to show the site preference of Te atoms via electronic band structure calculations in the framework of Korringa−Kohn−Rostoker[20−22] (KKR) method with coherent potential approximation (CPA) and neutron diffraction study on two $Mo_3Sb_{7-x}Te_x$ compounds with $x = 0$ and $x = 1.6$. We demonstrate that the partial exchange of antimony by tellurium is energetically more favorable on the 12d site, results further corroborated by Rietveld refinement on the neutron diffraction patterns. To further corroborate our theoretical statements, similar site energies calculations have been performed on the $Re_3As_{7-x}Ge_x$ system and were found to be in very good agreement with the neutron diffraction study previously reported by Soheilnia et al.[19] suggesting the 16f site preference of the Ge atoms. To go further, plotted density of states (DOS) of both the Te and Ge atoms on the 12d and 16f sites have been considered to try to elucidate the origin of such site preferences from an electronic point of view.

2. Experimental and Computational Details

Synthesis. Phases of nominal composition Mo_3Sb_7 and $Mo_3Sb_{5.4}Te_{1.6}$ were prepared by reaction of stoichiometric amounts of pure Sb powder (5NPlus, 99.999%), Mo powder (Cerac, 99.999%) and Te powder (5NPlus, 99.999%) in sealed evacuated quartz ampule under a He/H_2 atmosphere. The tubes were then tranferred into a programmable furnace and heated to 750 °C for 10 days. At the end of the process, the silica ampule was quenched in cold water. The solid products were then ground in an agate mortar into a fine powder (<100 μm) and further compacted into pellets in a steel die. To ensure good homogeneity of the samples, we annealed these pellets in a quartz ampule under a He/H_2

(18) Häussermann, U.; Elding-Ponten, M.; Svensson, C.; Lidin, S. *Chem. −Eur. J.* **1998**, *4*, 1007–1015.
(19) Soheilnia, N.; Xu, H.; Zhang, H.; Tritt, T. M.; Swainson, I.; Kleinke, H. *Chem. Mater.* **2007**, *19*, 4063–4068.
(20) Korringa, J. *Physica* **1947**, *13*, 392.
(21) Khon, W.; Rostoker, N. *Phys. Rev.* **1954**, *94*, 1111.
(22) Bansil, A.; Kaprzyk, S.; Mijnarends, P. E.; Tobola, J. *Phys. Rev. B* **1999**, *60*, 13396.

Table 1. Crystallographic Data from Neutron Diffraction Experiment on the Mo_3Sb_7 and $Mo_3Sb_{5.4}Te_{1.6}$ Compounds

	Mo_3Sb_7	$Mo_3Sb_{5.4}Te_{1.6}$
fw (g mol^{-1})	1140.1	1149.5
T (K)	298	298
space group	*Im3m*	*Im3m*
cell dimensions a (Å)	9.5692	9.5632
V (Å^3)	876.27	874.62
no. of formula units per cell	4	4
calcd density (g cm^{-3})	8.64	8.73
TOF range (μs)	2000−19000	2000−19000

atmosphere at 750 °C for 7 days. The final products were powdered again and densified by hot pressing in graphite dies in an argon atmosphere at 600 °C for 2 h under 51 MPa. The relative density, defined as the ratio of the measured density to the theoretical density, is 93 and 90% for the Mo_3Sb_7 and $Mo_3Sb_{5.4}Te_{1.6}$ compounds, respectively.

Crystal Structure and Chemical Analysis. X-ray powder diffraction (XRD) was performed on the ground materials obtained before the sintering process. The experiment was conducted with a Siemens D500 diffractometer using CoKα radiation and equipped with a curved primary beam monochromator and a linear detector (PSD). The X-ray diffraction pattern was recorded in the $\theta-2\theta$ mode between $20° \leq 2\theta \leq 110°$ with a 2θ step of 0.032° and a total counting time of 3 h. To obtain accurate lattice parameter, high-purity silicon ($a_0 = 5.4309$ Å) was added as an internal standard. Rietveld refinement against the XRD pattern did not enable us to differentiate tellurium from antimony. Therefore, to glean more information, we carried out neutron diffraction study.

EPMA analysis confirms the X-ray measurements as it reveals that both the Mo_3Sb_7 and $Mo_3Sb_{5.4}Te_{1.6}$ samples are homogeneous with a very good correlation between the real and nominal composition.

Neutron Diffraction. Neutron diffraction data were collected on 3 g of Mo_3Sb_7 and $Mo_3Sb_{5.4}Te_{1.6}$ powders on the time-of-flight diffractometer POLARIS at the ISIS facility, Rutherford Appleton Laboratory, U.K. ^{3}He tube detector banks at 35, 145, and the ZnS scintillation detector bank at 90° were used. This allows us to access an overall d-spacing spanning the range $0.3 \leq d \leq 8$ Å. Neutron data were acquired for 2 h at room temperature. The measurement was made for an integrated proton current at the production target of 200 μA h. The powder was contained in a vanadium cylindrical can. Rietveld refinement was carried out on the data using the Fullprof program using the 145° bank (backscattering detectors). The relevant crystallographic data from the neutron diffraction analysis are summarized in Table 1.

Electronic Structure Calculations. Electronic structure calculations of the $M_3X_{7-x}Y_x$ (M = Mo, Re; X = Sb, As; and Y = Te, Ge) system ($0 < x < 3$) have been performed by the Korringa-Kohn-Rostoker[20−22] method with the coherent potential approximation, where the chemical disorder has been treated as a random atom distribution. The description of the alloy including inequivalent sites can be better represented with the chemical formula $M_3(X1)_3(X2)_4$. In our computations, three types of X−Y disorder have been accounted for: a selective substitution either on the X1 site ($Mo_3Sb_{3-y}Te_ySb_4$) or on the X2 site ($Mo_3Sb_3Sb_{4-z}Te_z$) as well as a random distribution of Y atoms on both X sites ($Mo_3Sb_{3-y}Te_ySb_{4-z}Te_z$). Because of different multiplicities of the antimony sites, the relation $z = 3/4y$ has been employed in the random case. The self-consistent crystal potential of the muffin-tin form was constructed within the local density approximation (LDA) applying the Barth−Hedin formula for the exchange-correlation part. For well-converged charges and potentials, total, site-decomposed, and l-decomposed densities of states (DOS) were computed. The electronic structure of perfectly ordered compounds, Mo_3Sb_7 and $Mo_3Sb_4Te_3$, has also been considered by the full potential KKR calculations and detailed results are presented in the parallel work dedicated to the thermoelectric properties of some $Mo_3Sb_{7-x}Te_x$ compounds.[23] In this paper, we focus mainly on the electronic structure origin of the site-preference by comparing all contributions to the total energy (E_{tot}), basing our statements on KKR-CPA results as well as on plotted DOS. The lattice constants and positional parameters of Mo (12e) and Sb2 (16f) atoms used for computations were interpolated from the experimental crystallographic data, available for the $x = 0$ and 1.6 samples.

3. Results and Discussion

Structural Analysis. The X-ray diffraction pattern of the $Mo_3Sb_{5.4}Te_{1.6}$ compound is shown in Figure 2. This Te substituted compound crystallizes isotypic with the binary Ir_3Ge_7 structure type (space group *Im3m*) and no contributions from secondary phases can be observed. This feature suggests that all the tellurium has reacted and is consistent with previous studies reported on this system.[16,17] Whatever the sample is, neutron diffraction analysis was performed using the published XRD data on the Mo_3Sb_7 compound as a starting model. Because X-ray and EPMA analysis showed that both materials can be considered as single phase, no secondary phases were added in the model. Rietveld refinement of neutron time-of-flight diffraction pattern is represented in panels a and b in Figure 3 for Mo_3Sb_7 and $Mo_3Sb_{5.4}Te_{1.6}$, respectively. The refinement of the neutron data of Mo_3Sb_7 easily converged to a fully ordered atom arrangement with regard to the respective site distribution of Mo and Sb atoms and therefore led to good agreement factors (Table 2). The relevant parameters of this structure are listed in the Table 3. To study the possible site preference of tellurium in the $Mo_3Sb_{7-x}Te_x$ system, three models have been compared with either all the Te atoms located on the 12d site (i.e., 53.3% Te and 46.7% Sb), on the 16f site (i.e., 40% Te and 60% Sb) or on both sites (i.e., 26.6% Te and 73.4% Sb on the 12d site and 20% Te and 80% Sb on the 16f site). In each case, the structural parameters deduced from the Mo_3Sb_7 compound were used as the starting model and the overall composition was fixed by the EPMA analysis. The model dealing with the Te atoms located on the 12d site then leads to the best residual factors (Table 4). The difference in the three models studied is significant enough to conclude taking into account the similar scattering lengths of Sb and Te (Sb: +5.57 fm and Te: +5.80 fm), although this similarity precludes simultaneous refinement of the site occupancy factors and atomic displacement parameters. Crystallographic details including atomic positions and isotropic displacement parameters are summarized in Table 5. Selected bond lengths for these two compounds are available in the Supporting Information file. It is worth noticing that the presence of Te in the structure results in a slight decrease of the lattice parameter while the opposite trend has been reported for the $Re_3As_{7-x}Ge_x$ compounds.[19] As a conclusion, given the similarities in neutron scattering lengths of Sb and Te, the neutron diffraction provides evidence that Te atoms are only located on the 12d site. As

(23) Candolfi, C., et al. To be published.

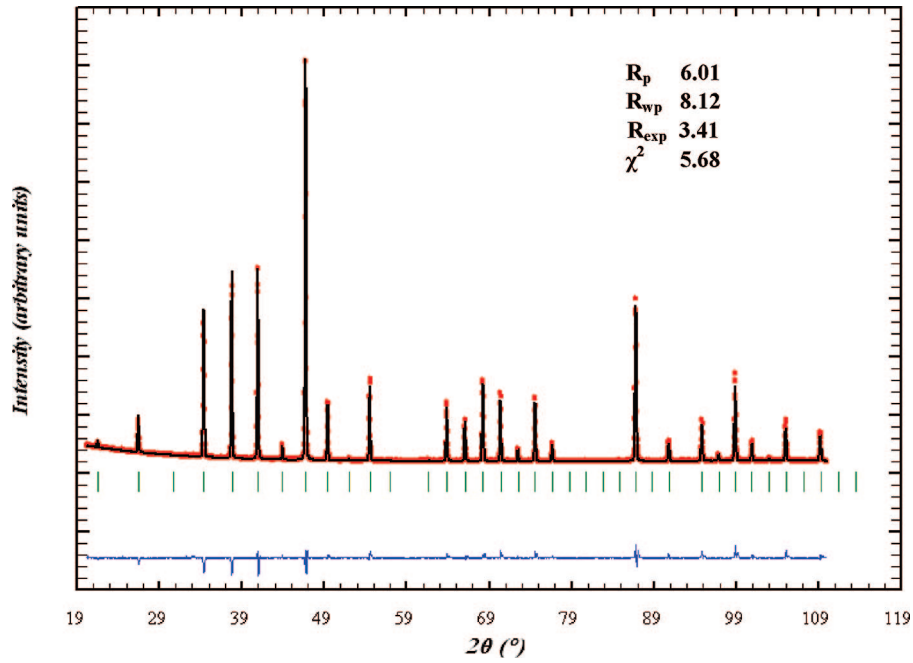

Figure 2. Rietveld refinement of the X-ray diffraction pattern of $Mo_3Sb_{5.4}Te_{1.6}$.

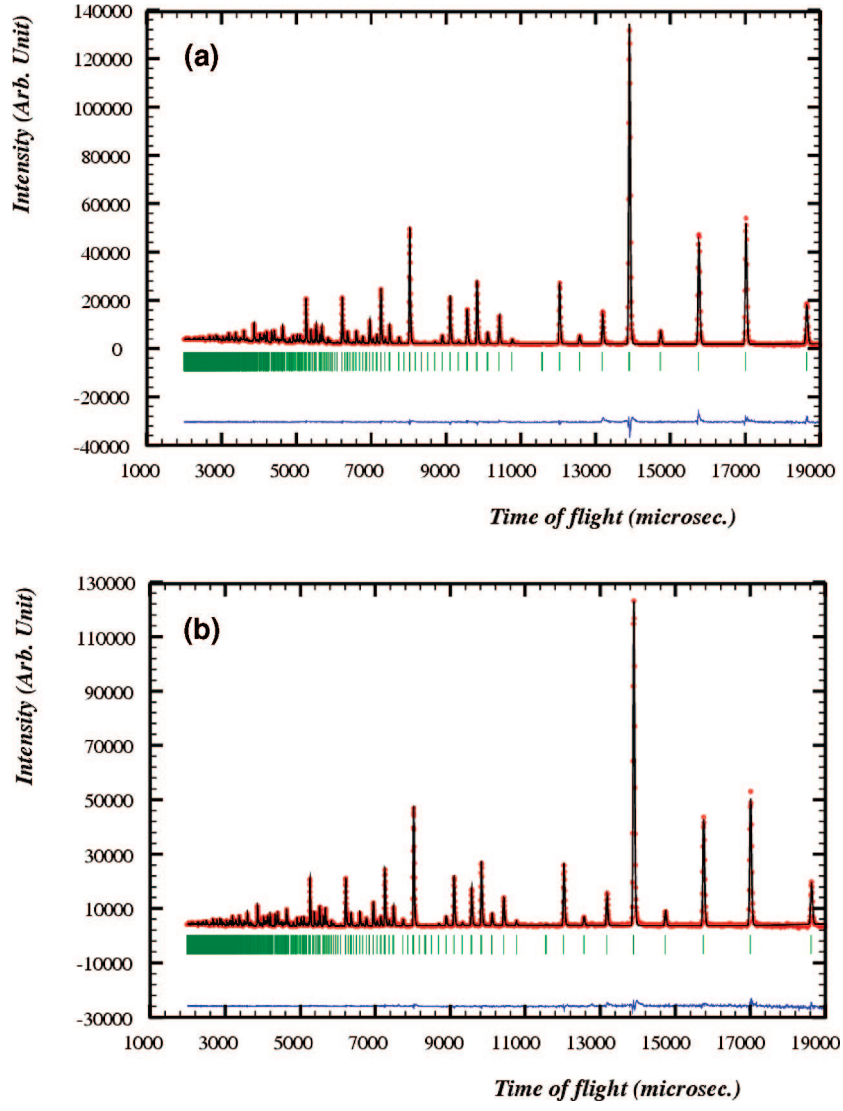

Figure 3. (a) Neutron diffraction pattern of the Mo_3Sb_7 compound. (b) Neutron diffraction pattern of the $Mo_3Sb_{5.4}Te_{1.6}$ compound.

Table 2. Agreement Factors of the Rietveld Analysis of the Mo_3Sb_7 Pattern

R_p	0.0278
R_{wp}	0.0217
R_{exp}	0.0130
χ^2	2.78

Table 3. Atomic Positions and Isotropic and Anisotropic Displacement Parameters (given in Å^2) of Mo_3Sb_7

atom	site	x	y	z	B_{iso} (Å)	occupancy (%)
Mo	12e	0.343(7)	0	0	0.31(2)	100
Sb1	12d	0.25	0	0.5	0.46(6)	100
Sb2	16f	0.162(4)	0.162(4)	0.162(4)	0.45(6)	100

	Mo	Sb1	Sb2
U_{11}	0.005(2)	0.003(8)	0.005(7)
U_{22}	0.003(3)	0.006(9)	0.005(7)
U_{33}	0.003(3)	0.006(9)	0.005(7)
$U_{12} = U_{13} = U_{23}$	0	0	0

Table 4. Agreement Factors of the Three Models Studied

	Te located on the 12d site	Te located on the 16f site	Te located on both sites
R_p	0.0231	0.0244	0.0240
R_{wp}	0.0182	0.0191	0.0189
R_{exp}	0.0120	0.0120	0.0120
χ^2	2.30	2.53	2.48

Table 5. Atomic Positions and Isotropic and Anisotropic Displacement Parameters (given in Å^2) of the Te-Substituted $Mo_3Sb_{5.4}Te_{1.6}$ Sample (Te atoms located on the 12d site)

atom	site	x	y	z	B_{iso} (Å^2)	occupancy (%)
Mo	12e	0.343(7)	0	0	0.25(6)	100
Sb1	12d	0.25	0	0.5	0.40(8)	46.7
Te1	12d	0.25	0	0.5	0.40(8)	53.3
Sb2	16f	0.162(8)	0.162(8)	0.162(8)	0.39(5)	100

	Mo	Sb1−Te1	Sb2
U_{11}	0.003(3)	0.003(3)	0.005(0)
U_{22}	0.003(2)	0.006(1)	0.005(0)
U_{33}	0.003(2)	0.006(1)	0.005(0)
$U_{12} = U_{13} = U_{23}$	0	0	0

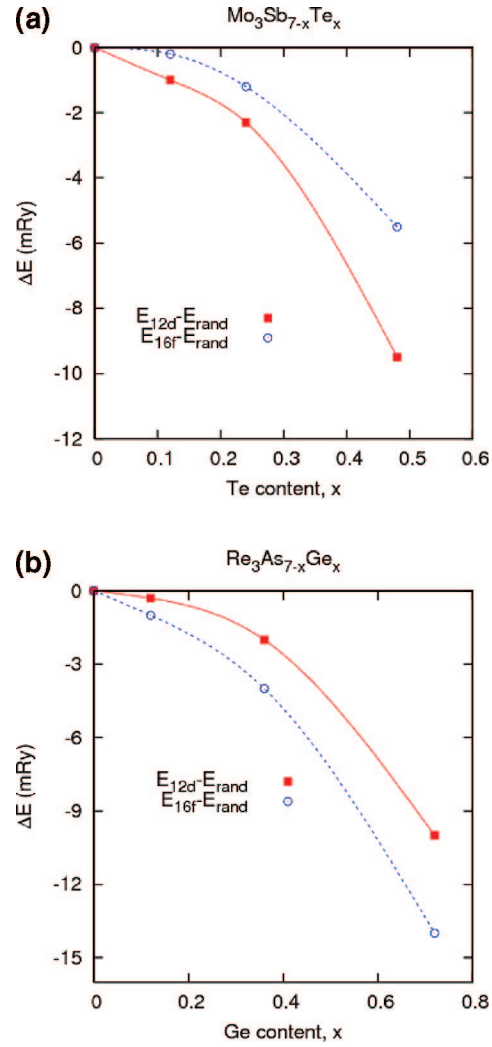

Figure 4. (a) Sb1 (12d) and Sb2 (16f) site energies as a function of the Te content. (b) As1 (12d) and As2 (16f) site energies as a function of the Ge content. For sake of clarity, the energy difference between a random configuration and a selective occupation has been considered.

we discuss below, band structure calculations seem to reinforce this picture.

Electronic Structure Calculations. The KKR-CPA total energies of disordered systems, where Sb1 (12d), Sb2 (16f), As1 (12d), and As2 (16f) were replaced (either preferentially or randomly) by Te and Ge in the $Mo_3Sb_{7-x}Te_x$ (Figure 4a) and $Re_3As_{7-x}Ge_x$ (Figure 4b), respectively, were calculated as a function of the Te and Ge content. In an effort to clearly observe even small variations, the energy difference, ΔE, between a random configuration (Te located on both sites corresponding to E_{rand}) and a selective occupation have been considered (E_{12d}, E_{16f}). These dependences unambiguously show that the higher the Te and Ge concentrations are, the higher is the energy difference between the two possible sites, the 12d site being energetically more favorable in the $Mo_3Sb_{7-x}Te_x$ compounds while the opposite behavior can be observed in the $Re_3As_{7-x}Ge_x$ system, i.e., a 16f site preference. Furthermore, these differences are significant enough even for low Te and Ge concentrations ($\sim$ 4 mRy for $x = 0.4$ and $\sim$ 2 mRy for $x = 0.4$, respectively) and clearly testifies to the site preference of these atoms. These results are in a very good agreement with the experimental evidence advanced by Soheilnia et al.[19] in the $Re_3As_{7-x}Ge_x$ system and in the present paper for the $Mo_3Sb_{7-x}Te_x$ system.

To try to better understand this behavior from an electronic point of view, we plotted the DOS contributions of Sb and Te atoms ($Mo_3Sb_{7-x}Te_x$ with x 0.12) in Figure 5a and of As and Ge atoms ($Re_3As_{7-x}Ge_x$ with $x \approx 0.25$) in Figure 5b for the 16f and 12d sites. The Sb contribution to the density of states at the Fermi level E_F is substantially higher on the 12d site whereas the Te DOS at E_F is quite small. This is in contrast with the 16f site where the Te contribution at E_F has almost the same value while the Sb one is strongly lower. Thus, substituting Sb atoms by Te atoms on the 12d site leads to stronger DOS decrease with respect to the 16f site. This could be the main reason of the higher decrease in the total energy when Te atoms are located on this site. Furthermore, comparing total number of valence electrons inside the muffin-tin spheres (both assumed to have strictly the same radius) around the 12d and 16f Sb sites, one finds an excess of about 0.1 electron in favor of Sb2 atoms. This behavior suggests the Sb1 local potential to be slightly more attractive with respect to the Sb2 one. In consequence, the 12d sites can favorably accommodate more electrons when

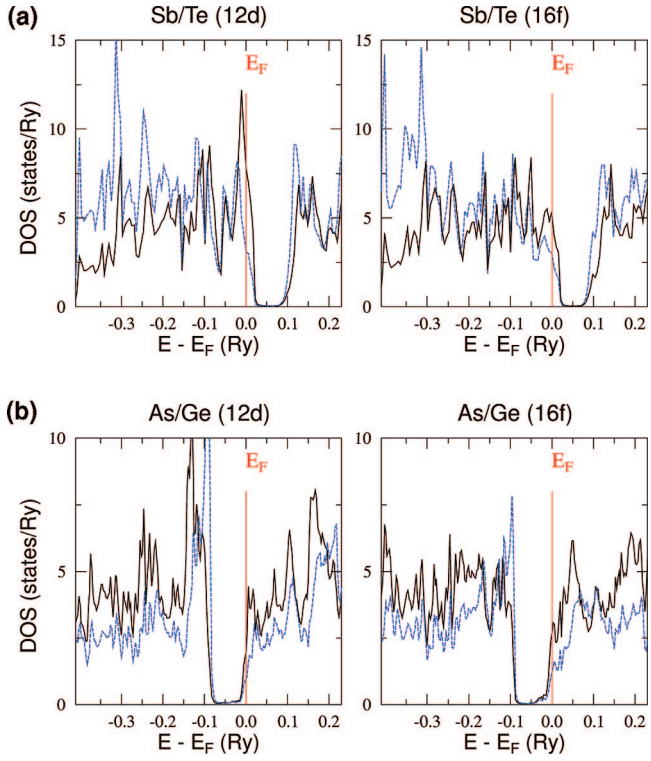

Figure 5. (a) DOS contributions of the Sb (solid black line) and Te atoms (dashed blue line) located on the 12d site and 16f site. (b) DOS contributions of the As (solid black line) and Ge atoms (dashed blue line) located on the 12d and 16f sites.

substituting antimony with more electronegative element as tellurium. This KKR-CPA result is in line with the predictions based on interatomic distance and chemical bonding analysis proposed by Dashjav et al.[16] They argued that Te (more electronegative than Sb) prefers a site with weaker homonuclear bonds, namely Sb1 (12d) squares, where the Sb1−Sb1 distance was as large as ∼ 3.38 Å. Conversely, in the case of Sb2 (16f) there is one shorter Sb2−Sb2 contact ∼ 2.9 Å connecting neighboring cubes formed by Sb2 atoms, which appears to be electronically unfavorable to be filled with additional electrons.

The reason for the 16f site preference in $Re_3As_{7-x}Ge_x$ is slightly different. Note that Re_3As_7 is a metal with the Fermi level located above the energy gap, leaving only one electron in the conduction band per formula. With increasing Ge concentration in $Re_3As_{7-x}Ge_x$, E_F tends to a low DOS energy region. Hence, in the case of As and Ge atoms, the situation is less evident as far as the site preference is concerned. Actually, if we carefully observe the DOS features near the Fermi level, comparable As and Ge DOS contributions can be distinguished. However, one can understand the 16f site preference by looking at the sharp DOS peak present just below the energy gap in both cases (Ge(12d) and Ge(16f)). Because these peaks strongly contribute to the total energy of the system, it appears to be energetically more beneficial for the $Re_3As_{7-x}Ge_x$ system to introduce Ge atoms on the 16f site rather than on the 12d site due to the substantially lower DOS peak. Like in $Mo_3Sb_{7-x}Te_x$, the muffin-tin spheres around As(16f) contain more electrons (∼0.06 *e)* than those around As(12d) atoms in the $Re_3As_{7-x}Ge_x$ system. Using similar chemical bonding arguments, one can expect that more electropositive Ge would tend to replace As on 16f site, where homonuclear As2−As2 bonds are stronger, which is again supported by our accurate KKR-CPA total energy and DOS analysis.

Conclusion

The $Mo_3Sb_{7-x}Te_x$ and $Re_3As_{7-x}Ge_x$ systems have been investigated from band structure calculations using the KKR-CPA method. In both systems, site preferences of the Te and Ge atoms have been clearly demonstrated. Although the 12d site is energetically more favorable in the $Mo_3Sb_{7-x}Te_x$ system, the $Re_3As_{7-x}Ge_x$ system displays the opposite feature, i.e., a 16f site preference. These theoretical results are experimentally corroborated by Rietveld refinement on the neutron diffraction patterns of $Mo_3Sb_{5.4}Te_{1.6}$ and Re_3As_6Ge reported in the present study and by Soheilnia et al.,[19] respectively.

Acknowledgment. C.C. greatly thanks M. Amiet and P. Maigné and acknowledges the financial support of the DGA (Délégation Générale pour l'Armement, Ministry of Defense, France) and the Network of Excellence CMA (Complex Metallic Alloys). J.T. acknowledges the support of the Polish Ministry of Science and Higher Education (Grant N202-2104-33).

Supporting Information Available: Tables of atomic distances for the Mo_3Sb_7 (Table 1) and $Mo_3Sb_{5.4}Te_{1.6}$ (Table 2) compounds (PDF). This material is available free of charge via the Internet at http://pubs.acs.org.

CM801560N